Research and Development of Electrodeless Plasma Thrusters Using High-Density Helicon Sources: The Heat Project

IEPC-2011-056

Presented at the 32nd International Electric Propulsion Conference,
Wiesbaden • Germany
September 11 – 15, 2011

S. Shinohara[1], H. Nishida [2], K. Yokoi[3] and T. Nakamura[4]
Tokyo University of Agriculture and Technology, Koganei, Tokyo 184-8588, Japan

T. Tanikawa[5]
Tokai University, Hiratsuka, Kanagawa 259-1292, Japan

T. Hada[6], F. Otsuka[7], T. Motomura[8], and E. Ohno[9]
Kyushu University, Kasuga, Fukuoka 816-8580, Japan

I. Funaki[10] and T. Matsuoka[11]
Japan Aerospace Exploration Agency, Sagamihara, Kanagawa 252-5210, Japan

and

K. P. Shamrai[12] and T. S. Rudenko[13]
Institute of Nuclear Research, Nauki, Kiev 03680, Ukraine

Abstract: **Although high specific impulse can be provided by electric propulsion systems, which are suited for long time missions, many of conventional electric thrusters suffer from a problem of finite life time due to the electrode wastage. In order to solve this problem, we have initiated the HEAT (Helicon Electrodeless Advanced Thruster) project to develop completely electrodeless advanced-concept electric thrusters. The entire process, i.e., a high-density (up to 10^{13} cm^{-3}) plasma production by helicon waves and its electromagnetic acceleration by some novel proposed methods, can be achieved without using any eroding electrodes. Here, as a review in our project, some experimental and theoretical approaches to realize this concept are presented.**

[1]Professor, Institute of Engineering, sshinoha@cc.tuat.ac.jp
[2]Associate Professor, Institute of Engineering, hnishida@cc.tuat.ac.jp
[3]Graduate Student, Graduate School of Engineering
[4]Graduate Student, Graduate School of Engineering, 50010643508@st.tuat.ac.jp
[5]Professor, Research Institute of Science and Technology, tnth@keyaki.cc.u-tokai.ac.jp
[6]Professor, Interdisciplinary Graduate School of Engineering Sciences, hada@esst.kyushu-u.ac.jp
[7]Postdoc, Interdisciplinary Graduate School of Engineering Sciences, otsuka@esst.kyushu-u.ac.jp
[8]Graduate Student, Interdisciplinary Graduate School of Engineering Sciences, tmoto@aees.kyushu-u.ac.jp
[9]Graduate Student, Interdisciplinary Graduate School of Engineering Sciences, mikuro0602@gmail.com
[10]Associate Professor, Institute of Space and Astronautical Science, funaki@isas.jaxa.jp
[11]Researcher Fellow, Institute of Space and Astronautical Science, takeshi.matsuoka1@gd.isas.jaxa.jp
[12] Head, Department of Plasma Theory, kshamrai@kinr.kiev.ua
[13] Graduate Student, rudenkot@kinr.kiev.ua

Nomenclature

a	=	plasma radius
B	=	axial component of the static magnetic field
B_0	=	magnetic field at the ion cyclotron resonance in the ICR/PA scheme
B_a	=	axial component of the static magnetic field near the antenna
B_{MP}	=	magnetic probe signal of the RMF magnetic field
B_r	=	radial component of the static magnetic field
B_{RMF}	=	magnetic field generated by RMF coil current
E_0	=	maximum electric field in the ICR/PA scheme
E_{rf}	=	rf electric field applied in the ICR/PA scheme
$E_\perp$	=	transverse electric field applied in the REF scheme
f	=	excitation rf frequency for the plasma production
f_{RMF}	=	RMF excitation frequency
I_{RMF}	=	RMF current in the coils
I_{sp}	=	specific impulse
j_θ	=	azimuthal component of the induced current density
$k_{//}$	=	parallel wavenumber
L_A	=	axial scale length of acceleration region in the RMF scheme
L_B	=	axial scale length of the magnetic field in the ICR/PA scheme
L_E	=	axial scale length of the rf electric field in the ICR/PA scheme
L_p	=	axial plasma length
m	=	mass of ion
n_e	=	electron density
N_e	=	total number of electrons in the whole plasma
P_{Ar}	=	argon pressure
P_{inp}	=	rf input power for plasma production
P_{RMF}	=	RMF input power
q	=	ion charge
r	=	radial position in the cylindrical coordinate
R_D	=	$E_r / \omega B$
R_L	=	v_0 / ω_{ce} (electron gyro radius)
T_e	=	electron temperature
v	=	ion flow velocity
v_0	=	electron velocity in the REF scheme
v_b	=	initial parallel ion velocity to the axial magnetic field
v_z	=	parallel ion velocity to the axial magnetic field
z	=	axial position in the cylindrical coordinate
z_{res}	=	axial position of the ion cyclotron resonance in the cylindrical coordinate
δ	=	skin depth
$\Delta\varepsilon$	=	increment of ion energy
$\varepsilon_{//}$	=	parallel ion energy
$\varepsilon_\perp$	=	perpendicular ion energy
γ	=	ω_{ce} / ν (Hall parameter)
η	=	plasma resistivity
λ	=	a / δ (reciprocal of the normalized skin depth)
ω	=	angular excitation frequency in RMF, REF, and ICR/PA schemes
ω_{ce}	=	electron cyclotron angular frequency in the REF scheme
ω_{ce}'	=	electron cyclotron angular frequency defined by using RMF strength
Ω_{ci}	=	ion cyclotron angular frequency

I. Introduction

HIGHER specific impulse I_{sp} can be provided by electric propulsion systems compared to chemical ones, and the high I_{sp} enables a long time duration mission such as a deep space exploration. The first successful asteroid sample return mission by the Japanese “Hayabusa” spacecraft[1,2] could not have been achieved without the μ-10 ion engines, one type of electric thrusters. However, present-time electric plasma thrusters,[3] ion engines included, suffer from a problem of finite lifetime due to the erosion of various electrodes that are in direct contact with plasmas. In order to solve this problem, several novel methods[3] are proposed, mostly using helicon plasma sources[4,5]: e.g., Variable Specific Impulse Magnetoplasma Rocket (VASIMR),[6] Mini-Magnetospheric Plasma Propulsion (M2P2)[7] based on the Magsail concept,[8] Helicon Ion Thruster,[9] and Double Layer (DL) Thruster,[10] including ours.[11-18]

Here, we have initiated the HEAT (Helicon Electrodeless Advanced Thruster) project to develop completely electrodeless advanced-concept electric thrusters. In our scheme, source dense plasmas (electron density n_e up to 10^{13} cm^{-3}) in insulation tubes are produced extremely efficiently using helicon waves with a radio-frequency (rf) range between ion and electron cyclotron frequencies; they are then electromagnetically accelerated to a high velocity to yield a thrust. The entire process can be achieved without using any eroding electrodes, which are located on the outside of the insulation tube, leading to electric thrusters with a limitless lifetime.

In this paper, as a review in our project to realize completely electrodeless plasma thrusters, after introducing high-density helicon plasma sources developed, we will present some experimental and theoretical approaches of a propulsion scheme: 1) a Rotating Magnetic Field (RMF) acceleration, based on the Field Reversed Configuration (FRC) concept in a fusion field,[19] 2) a Rotating Electric Field (REF) or a Lissajous acceleration,[11,12,15-18] which will be also presented in detail in this conference[20,21] [see left- and right-hand sides in Fig. 1, respectively], and 3) the ion cyclotron resonance (ICR) acceleration with a ponderomotive force acceleration (PA) (a configuration of the numerical calculation in this scheme will be shown later in Fig. 11).

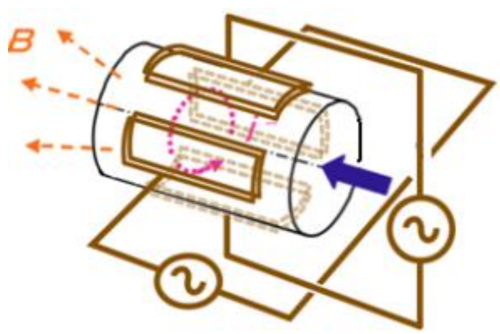

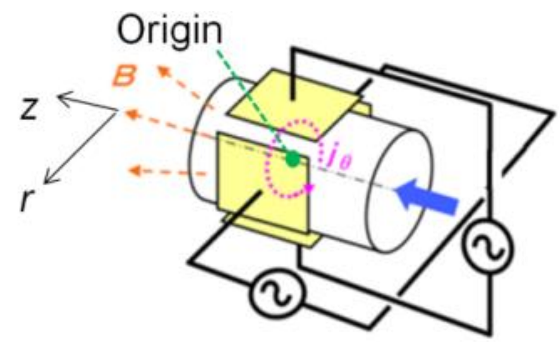

Figure 1. Configurations of (left) the RMF and (right) REF acceleration. schemes.

II. High-Density Helicon Plasma Production

Here, we will briefly show our development of high-density helicon plasma sources up to seven ones.[15] Figure 2 shows a dispersion relation of the helicon waves under a uniform electron density.[5] Here, f, B, a, and $k_{//}$ show the excitation frequency, the axial component of the static magnetic field, plasma radius, and parallel wavenumber, respectively. It can be seen that with the increase in $k_{//}$ (decrease in a), the ordinate, i.e., fn_e/B, increases.

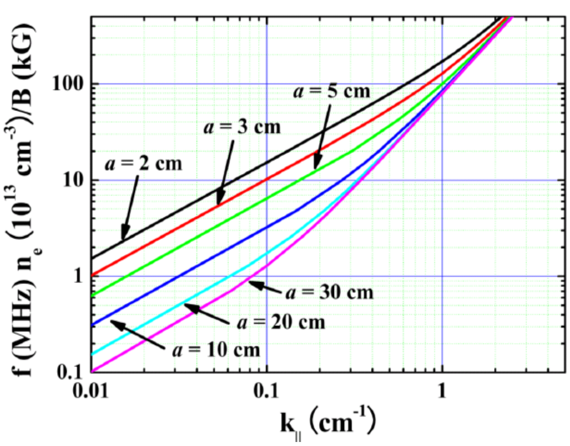

Figure 2. Dispersion relation of helicon waves.

Figure 3 shows an example of the experimental results, i.e., n_e as a function of the rf input power P_{inp}, using the developed Large Helicon Plasma Device (LHPD)[22] at the Institute of Space and Astronautical Science / Japan Aerospace eXploration Agency (ISAS/JAXA) in the case of the axial plasma length L_p is 81 cm. Here, the machine inner diameter (i.d.) and the axial length are 74 cm, and 486 cm, respectively, and a spiral antenna for the large diameter plasma production is used. With the increase in P_{inp}, n_e inceases: the discharge mode changes from Capacitively Coupled Plasma (CCP) to Helicon Plasma (HP) through Inductively Coupled Plasma (ICP). It can be also seen that the increase in the static magnetic field (axial component) near the antenna B_a, which is controlled by the the coil current near the antenna, the minimum P_{inp} to have a density jump from ICP to HP increases (in this figure, I_c = 20, 40, 60, and 80 A in the cases of red open circles, blue open boxes, green closed diamonds, and black open triangles, respectively).

In the case of a long cylinder plasma sources with a small diameter and weak magnetic field, N_e/P_{inp} is expected to be proportional to a^2 from the classical diffusion (mainly the radial diffusion in this case), where N_e is a total number of electrons in a whole plasma.[23] As shown in Fig. 4, this scaling, showning an theoretical upper limit of a plasma production, holds good in a wide range of the plasma radius.[15] Here, red closed circles are obtained in our group: the largest one is LHPD (plasma volume is up to 2.1 m^3),[22] denoted as “present device” in Fig. 4, and the smallest source has been also developed: i.d. is 2.5 cm (L_p can be lowered to 4.7 cm, which shows the smallest volume of 23 cm^3).[11]

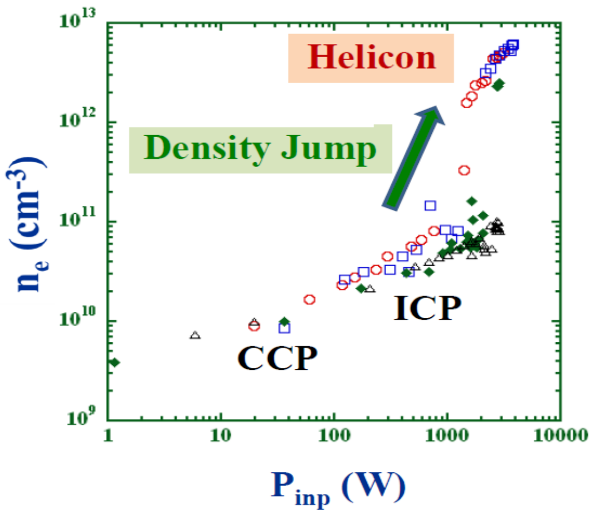

Figure 3. Electron density n_e as a function of the rf input power P_{inp}, changing the magnetic field near the antenna B_a.

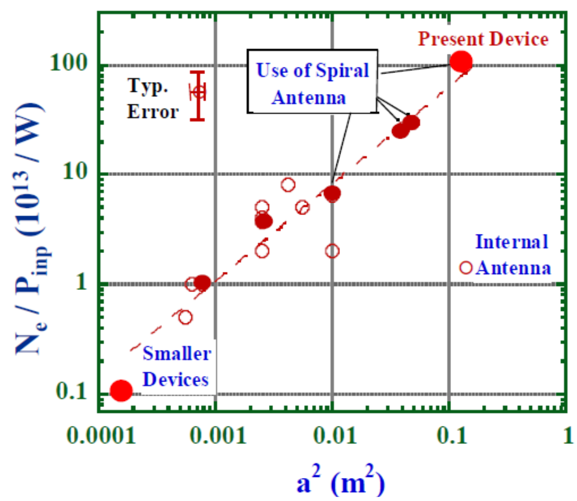

Figure 4. N_e/P_{inp} vs a^2 for different helicon sources. Here, red closed circles show the data taken by our group.

The axial plasma length L_p is important regardless of plasma sources, and we have succeeded in the high-density plasma production in the LHPD, changing L_p by using various types of the termination plates: In the longest (shortest) case, n_e is close to 10^{13} (10^{12}) cm^{-3} with L_p = 486 (5.5) cm with P_{inp} < 4 kW. In the case of the short cylinder plasma sources with the large diameter and the strong magnetic field, which is contrary to the case shown in Fig. 4, N_e/P_{inp} is expected to be proportional to L_p from the classical diffusion (mainly the axial diffusion in this case).[23] Experimental data of the relation between N_e/P_{inp} and L_p also show a good agreement with the expectation as well as showing a good production efficiency (not shown).

From our helicon high-density plasma sources developed, helicon sources in a wide range of scales are found to be very useful in applying to the next generation (substantial) electrodeless thrusters.

III. Acceleration Schemes

In this section, we will present three proposed acceleration schemes, i.e., RMF, REF, and ICR/PA, with the acceleration electrodes being indirect contact with the plasma, leading to a longer life time operation due to the reduction of the strong plasma interaction with the materials.

The former two schemes of RMF and REF are expected to exhaust the plasma with the electromagnetic force, i.e., $j_\theta \times B_r$, in the presence of the static divergent magnetic field. Here, j_θ and B_r are induced azimuthal current density by external electrodes based on the proposed schemes, and the radial component of the static magnetic field, respectively, in the cylindrical coordinate. The RMF and REF vectors (radial magnetic and electric fields, respectively) lie in the cross sectional plane of the plasma and rotate with the drift motion at applied RMF and REF frequencies (under the immobile ion assumption), respectively, around the z axis. This electron drift is the source of the j_θ (refs. 11 and 19). On the other hand, ICP/PA scheme utilizes the asymmetric oscillating electric field in the divergent magnetic field, which will be shown later.

Here, these three schemes will be described in detail. Note that, in each scheme, we wish to stress that “nonlinearity” is a key issue in electrodeless plasma acceleration of any sort. This is evident since only time-dependent electromagnetic perturbations (such as rf waves) can penetrate into the plasma to cause its motion, while the net dc thrust should not vanish by time averaging, suggesting that a nonlinear coupling of two ac signals must produce a dc output. According to a conventional wisdom, “nonlinear” means “weak”, and thus it is a challenge to generate a large dc power output out of externally applied ac fields (or waves).

A. RMF Scheme

The initial RMF experiments have been carried out using the Large Mirror Device (LMD),[24] as shown in Fig. 5. The RMF coils (10 turns) are mounted on the quartz glass tube (5 cm i.d. and 50 cm length), which is inserted into the vacuum chamber. To generate a helicon plasma to be accelerated by the RMF scheme, a single loop antenna of 4 cm in width is also installed. The rf input power P_{inp} and the excitation frequency f are ~ 2 kW and 7 MHz (for the plasma production), and P_{RMF} < 1 kW and f_{RMF} = 1 MHz (for the RMF method), respectively. Radially movable standard and directional Langmuir probes at the axial position of z = 15 cm are used to measure the electron density and the ion flow velocity, respectively. In order to measure the RMF penetration, which is essential in this scheme,[25] a magnetic probe is placed in the center of the RMF coils. Here, the argon gas pressure P_{Ar} is 0.75 mTorr, which is important from a viewpoint of the collision frequency ν (the summation of electron-ion and electron-neutral collision frequencies), and the electron temperature T_e is typically ~3 eV.

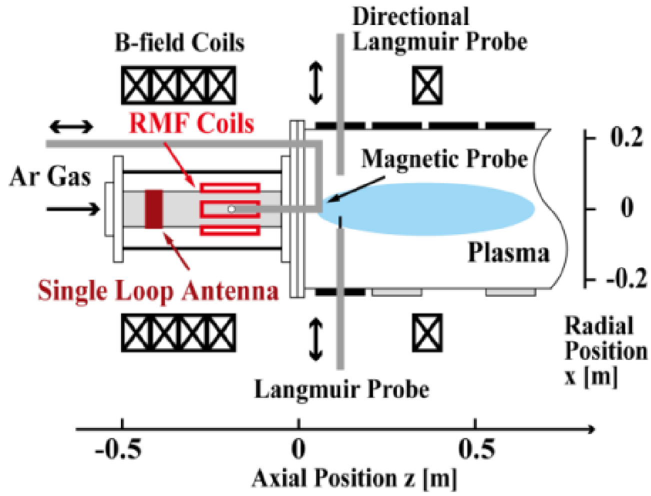

Figure 5. Experimental setup for RMF scheme in LMD.

As was mentioned, the penetration of the RMF is important and its penetration conditions are determined by the following two parameters[25]: $\gamma = \omega_{ce}' / \nu$ (the Hall parameter) and $\lambda = a / \delta$ (a reciprocal of the normalized skin depth). Here, ω_{ce}' and δ are an electron cyclotron angular frequency defined by using the RMF strength B_{RMF} and a skin depth, respectively. In order to have a full penetration, a higher value of γ / λ (e.g., > 1.12 for λ < 6.5) are required,[25] showing that the larger B_{RMF} and smaller n_e, f_{RMF}, a, P_{Ar} and η (plasma resistivity) are necessary. On the other hand, a plasma thrust[26] is proportional to n_e, f_{RMF}, B_r, and a^3 (see also a thrust discussion shown below), which is contradictory to the above penetration condition, and experimentally we must make a compromise between two conditions of the penetration and the thrust.

Here, we will discuss the thrust in this RMF scheme. In the case of the full penetration of the RMF, the electrons make a rigid rotation, so that the electron density is given by $j_\theta = n_e e r \omega$, where $\omega = f_{RMF} / 2\pi$. If the B_r is expressed as ~ B_z $(r / 2R)$ (in the divergent magnetic field region just outside the magnetic field coil with its radius of R) and the electron density is spatially uniform, then the thrust can be estimated as,

$$F = L \int_0^a j_\theta \; B_r \; (2\pi r) \; dr = \frac{\pi a}{4R} e \; n_e \; L_A \; \omega \; B_z \; a^3, \qquad (1)$$

where L_A is the axial length of the accelerating region. For typical values of $\omega = 6 \times 10^6$ s^{-1}, R ~ a = L_A = 0.05 m, n_e = 10^{18} m^{-3}, and B_z = 0.05 T, Eq. (1) yields F ~ 100 mN, which is enough for the thrust value. We note that the thrust is not reduced significantly even if the RMF penetration is partial, since the thrust is mainly reduced by the current near the edge of the plasma.

In our experiments, we have surveyed the helicon plasma performance to have a high-density up to ~ 10^{13} cm^{-3} in the source region by changing B_z, the magnetic field configuration (the field divergence is important), and P_{Ar}. Especially, lowering P_{Ar} to have a lower η is tried to satisfy the field penetration condition, and we must note that n_e is lower in the acceleration region compared to the source region due to the divergent magnetic field in the

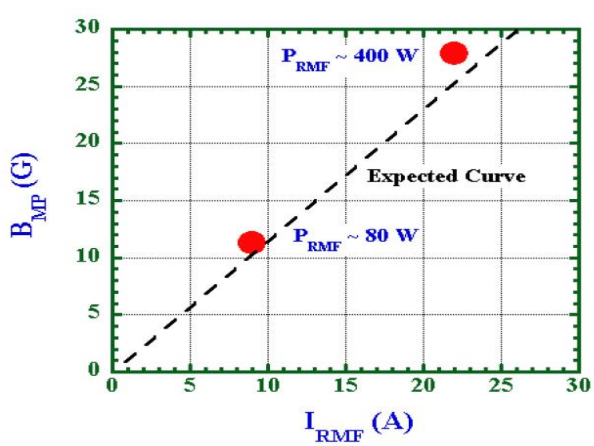

Figure 6. Magnetic probe signal B_{MP} vs. RMF current I_{RMF}.

downstream.

Figure 6 shows the initial result of the RMF penetration that is essential to induce the nonlinear j_θ. The ordinate is the magnetic field strength measured by using the magnetic probe, B_{MP}, with f_{RMF} = 1 MHz. The abscissa is the RMF coil current, I_{RMF}. It can be seen from this figure that the full penetration of the RMF is achieved at the points of I_{RMF} ~ 9 A and 22 A. This B_{MP} is in good agreement with the expected curve (a dashed line), using the RMF coil current in the absence of the plasma. This result is supported by the theoretical results in Refs. 25 and 26. Preliminary measurement of the plasma flow is also done by applying the RMF, using a Mach probe,[27,28] and a small increment of the Mach flow velocity M by < 0.3 along with the increment of n_e is found.

Theoretical approach for RMF to describe the thrust has been also done, using the two important dimensionless parameters: normalized plasma radius and the electron Hall parameter, which is influenced by the resistivity. For further studies, we need to consider the following processes using fluid or kinetic plasma treatments: 1) RMF penetration and induced current channel, 2) spin-up time scale of the plasma rotation, 3) electron axial flow and electron transit time normalized by the $1 / f_{RMF}$, 4) plasma acceleration via electron current, and 5) plasma detachment.

B. REF Scheme

Next, we will briefly describe the REF (Lissajous) scheme, since this will be presented in detail in other papers,[20,21] as was mentioned. The principle of this acceleration can be explained using a two-dimensional electron trajectory analysis. Here, two circular motions, whose radii are given by $R_D = E_\perp / \omega B$ and the electron gyro radius $R_L = v_0 / \omega_{ce}$ play important roles in the calculation ($E_\perp$: transverse electric field, v_0: electron thermal velocity, ω_{ce}: electron cyclotron angular frequency). Figure 3 shows schematic pictures of (left) the electron trajectory and (right) the induced electron current in this scheme.

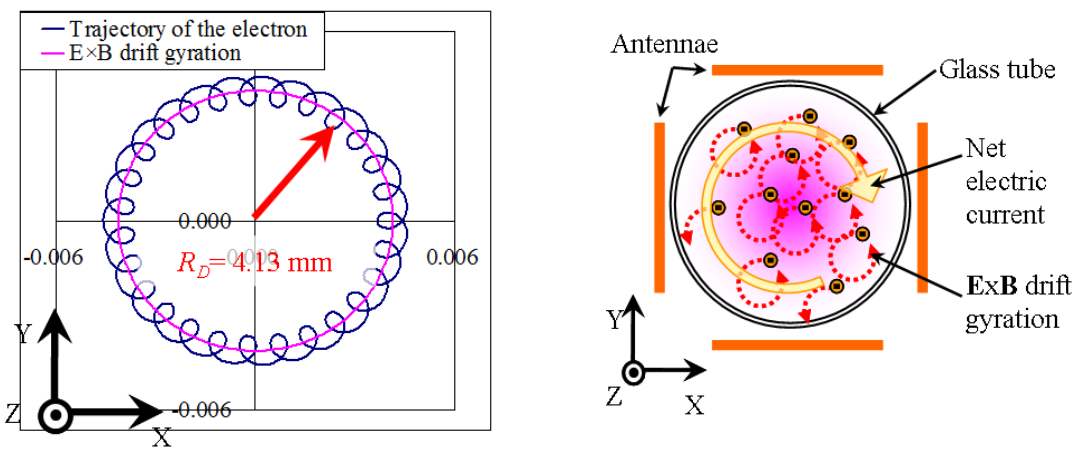

Figure 7. (left) Trajectory of the electron under REF and uniform magnetic field: R_L/R_D = 0.11 and ω_{ce}/ω = 28. (right) Induction of azimuthal electric current by superposition of the Ex×B gyration motions.

Here, we have developed a small helicon plasma source for acceleration experiments using this REF scheme,[14,17] as shown in Fig. 8. A glass tube, 2.5 cm i.d. and the total axial length of ~ 40 cm, is connected to a vacuum chamber. A double saddle type antenna is used for the helicon plasma production, and the two pairs of flat plate electrodes are used to apply the REF for the plasma acceleration. The excitation frequencies for both the plasma production and acceleration are fixed at 27.12 MHz,

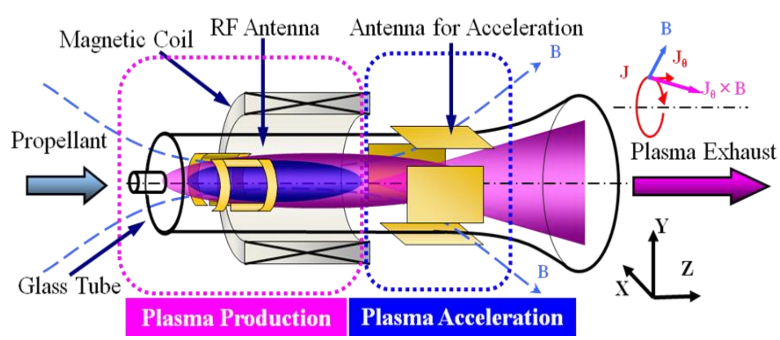

Figure 8. Schematic of REF method using a helicon source.

and the net-absorbed powers of the plasma production and acceleration are 290 W and 125 W, respectively. The argon gas pressure P_{Ar} in the expansion chamber is fixed at ~ 0.4 mTorr. The para-perp type Mach probe[29] is used to measure the ion flow velocity v, T_e, and n_e.

The radial profile of v is shown in Fig. 9 with a phase change of 120° between two electrodes. The closed triangles and crosses show the results before and after applying the REF, respectively. It can be seen that v is increased in the plasma central region after applying the REF. In addition, n_e (T_e) is decreased (increased) in the plasma central region (not shown). In order to measure the thrust, we have also a developed a high-density helicon source, 2.6 cm i.d. with a one-turn loop, in the vacuum chamber of the LHPD.[15,22] Figure 10 shows an example of the initial measurement of the thrust by using a thrust stand, changing the mass flow rate along with a plasma emission. Although the optimization is necessary for target plasmas to be applied by the REF method, this shows that with the increase in a mass flow rate, a thrust increases, on the order of ~ mN, where I_{sp} ~ 100-200 s.

The REF penetration into the dense plasma has been calculated. The j_θ is found to be proportional to the R_D/a up to an optimum value of R_D/a ~ 0.4, then j_θ decreases after this optimum value ~ 0.4 due to the particle loss to the wall. The REF strength from a 1D analytical model is compared with the results from 1D PIC simulations carried out by using the VORPAL code,[30] and the REF penetration results are in good agreement. Furthermore, a parameter survey of the thrust force has been done based on the above calculation, changing external parameters such as a, ω, B and n_e.

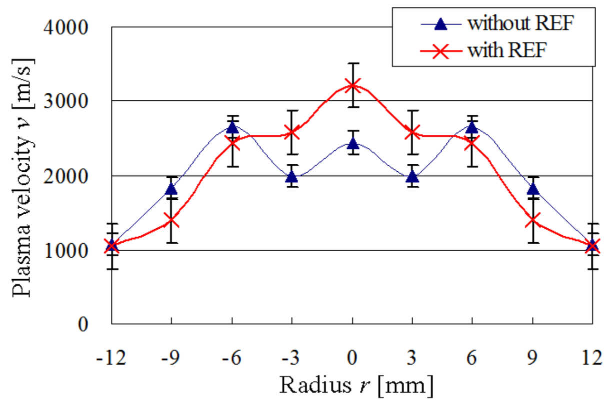

Figure 9. Ion flow velocity profile at 50 mm downstream

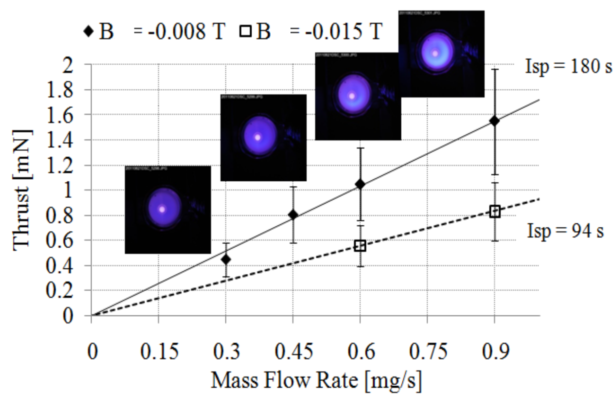

Figure 10. Correlation between a plasma emission and a thrust, changing a mass flow rate.

Further studies are necessary such as 1) an optimization of an applied electrodes position and their numbers, 2) control of a collision frequency and an electron density profile, 3) electron axial diffusion and electron transit time normalized by by the $(2\pi/\omega)$, 4) plasma acceleration via electron current, 5) plasma detachment, along with a 2D or 3D analysis as to the electric field penetration in order to verify this scheme.

C. ICR/PA Scheme

Here, we will discuss ICR/PA method (see Fig. 11). In this scheme, the ions can be efficiently heated perpendicularly by ICR. In the divergent field, as the ions travel into a region with weaker magnetic field, their perpendicular energy can naturally be converted into the parallel energy, producing the thrust.[31] In addition, by applying the rf waves in such a way that the resonance point coincides with the peak of the wave energy density, the ions can gain parallel acceleration due to the electromagnetic ponderomotive force.[32,33] The ICR and the PA are inseparable, yet the latter is

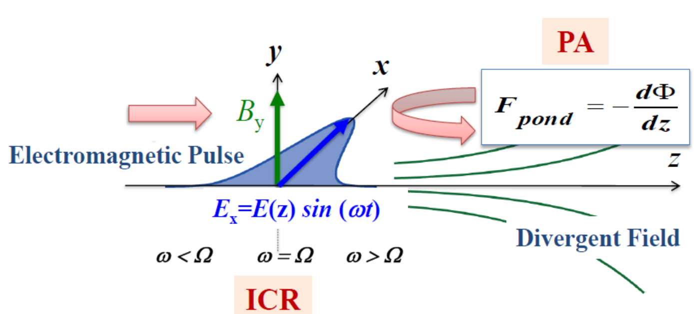

Figure 11. Concept of ICR/PA scheme.

preferred since it is less likely to be influenced by the ion-wall interaction (due to the smaller gyro radius). The thrust by this scheme has been formulated with ions crossing the region of the ponderomotive potential, which is written as $(q^2/4m)\,[E_{rf}^{\ 2}/(\omega^2 - \Omega_{ci}^{\ 2})]$. Here, q, m E_{rf}, ω, and Ω_{ci} are ion charge, mass of ion, rf electric field applied depending on position, applied angular frequency of this electric field, and ion cyclotron angular frequency.

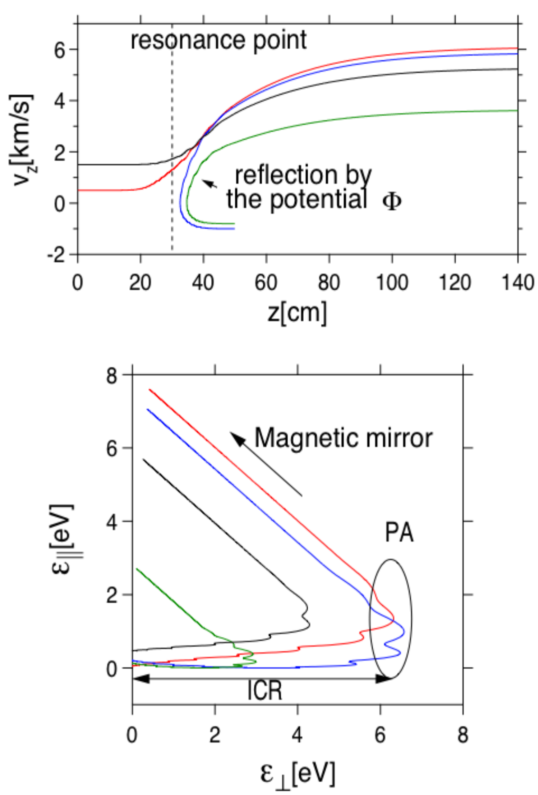

Figure 12. (top) Ion trajectory in (z, v_z) plane and (bottom) increment of ion energy in ($\varepsilon_{\perp}$, $\varepsilon_{//}$) plane.

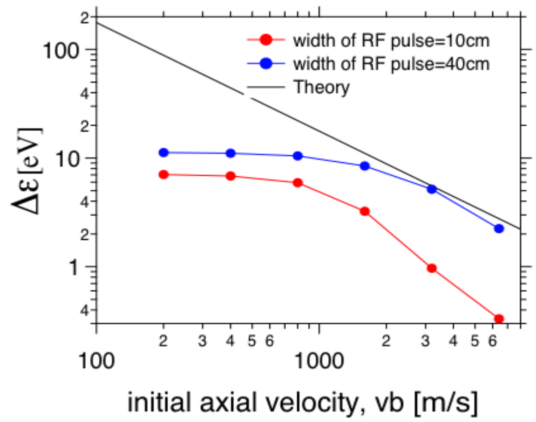

Figure 13. Increment of ion energy $\Delta\varepsilon$ as a function of the initial axial ion velocity v_b, changing the width of RF pulse width L_E along with a theoretical line.

Figure 12 shows a typical example of (top) the ion trajectory and (bottom) energy increment in ($\varepsilon_{\perp}$, $\varepsilon_{//}$) plane in this ICR/PA scheme by changing the initial parallel velocity v_b (blue, green, red, and black lines show -1,000, -800, 500, 1,200 m/s, respectively). Here, $\varepsilon_{//}$ and $\varepsilon_{\perp}$ shows the parallel and perpendicular ion energies to the axial magnetic field, respectively. The increment of the ion energy $\Delta\varepsilon$ is summarized in Fig. 13, changing the rf pulse width L_E {z direction, whose definition is shown in Eq.(2)}, along with a thoeretical line[30] expressed as $\Delta\varepsilon = (\pi q^2 E_0^{\ 2}/4m)\,(L_B/\omega v_b)$, where E_0 is the maximum rf electric field and L_B is the axial scale length of the magnetic field {see Eq.(2)}, assuming only the ICR mechanism and a fixed parallel velocity. Here, the electric and the magnetic fields are written as follows (z_{res}: axial position of the ion cyclotron resonance, B_0: magnetic field at the ion cyclotron resonance position z_{res}).

$$E(z) = E_0 exp\left(-\frac{(z-z_{res})^2}{L_E^2}\right), \quad B(z) = B_0\left(1 + tanh(-\frac{z-z_{res}}{L_B})\right) \quad . \tag{2}$$

From this figure, it can be seen that the PA adds the incremental energy done by ICR alone.

Now, we have initiated the proof of principle experiment in this scheme using the Tokai Helicon Device (THD),[34] considering a collision and a plasma-wall interaction.

IV. Conclusion

In order to realize completely electrodeless plasma thrusters, we have initiated the HEAT project by some novel methods: the entire process of the plasma production by the helicon waves and the electromagnetic acceleration can be achieved by the external electrodes which are not in direct contact with the plasmas, causing a long life time. Here, as a review in our project, some experimental and theoretical approaches are presented and discussed: high-density plasma production by the helicon waves, and proposed acceleration methods of RMF, REF, and ICR/PA.

In order to verify the proposed schemes, we need further studies on the above methods along with new measurements such as by using electrostatic probes (sophisticated Langmuir and Mach probes as well as an ion energy analyzer) and magnetic probes, and by optical instruments (a diode laser for laser induced fluorescence method, a fast camera, and a monochromator) with thrust measurements.

Acknowledgments

The authors would like to thank late Prof. Kyoichiro Toki for their great contribution to our project, and dedicate this paper to the memory of him. We would also like to thank Prof. Fujino and Mr. Satoh in carrying out the thrust measurement using a small helicon source. This work has been partly supported by the Grants-in Aid for Scientific Research under Contract No. (S) 21226019 from the Japan Society for the Promotion of Science.

References

[1]Kuninaka, H., and Satori, S., "Development and Demonstration of a Cathodeless Electron Cyclotron Resonance Ion Thruster", *J. Propul. Power*, Vol. 14, No. 6, 1998, pp.1022-1026.

[2]Kuninaka, H., Nishiyama, K., Funaki, I. Yamada, T., Shimizu, Y., and Kawaguchi, J., "Powered Flight of Electron Cyclotron Resonance Ion Engines on Hayabusa Explorer", *J. Propul. Power*, Vol. 23, No. 3, 2007, pp.544-551.

[3]Charles, C., “Plasma for Spacecraft Propulsion,” *J. Phys. D: Apply. Phys.*, Vol. 42, No. 16, 21 Aug. 2009, pp. 163001 1-18. (Topical Review Paper)

[4]Boswell, R. W., “Plasma Production Using a Standing Helicon Wave,” *Phys. Lett.*, Vol. 33A, No. 7, 14 Dec. 1970, pp.457-458.

[5]Shinohara, S., “Propagating Wave Characteristics for Plasma Production in Plasma Processing Field,” *Jpn. J. Appl. Phys.*, Vol. 36, Part I, No. 7B, 1997, pp. 4695-4703. (Review Paper)

[6]Chang –Díaz, “The VASIMR Rocket,” *Sci. Am.*, Vol. 283, Nov. 2000, pp.90-97.

[7]Winglee, R. M., Slough, J., Ziemba, T., and Goodson, A., “Mini-Magnetospheric Plasma Propulsion: Tapping the Energy of the Solar Wind for Spacecraft Propulsion,” *J. Geophys. Res.*, Vol. 105, No. A9, 2000, pp. 21067-21077.

[8]Zubrin, R. M., and Andrews, G. A., “Magnetic Sails and Interplanetary Travel,” *J. Spacecraft*, Vol. 28, No. 2, Mar.-Apr. 1991, pp. 197-203.

[9]Shamrai, K. P., Aleksandrov, A. F., Bougrov, G. E., Virko, V. F., Katiukha, V.P., Koh, S. K., Kralkina, E. A., Kirichenko, G. S., and Rukhadze, A. A., “Quasistatic Plasma Sources: Physical Principles, Modelling Experiments, Application Aspects,” *J. Phys. IV France, Colloque C4, Suppl ément au Journal de Physique III*, Vol. 7, Oct. 1997, pp. C4 365-381.

[10]Charles, C., Boswell, R. W., Bouchoule, A., Laure, C., and Ranson, P., “Plasma Difusion from a Low Pressure Radio Frequency Source,” *J. Vac. Sci. Technol.*, Vol. A 19, Issue 3, 1991, pp. 661 – 663.

[11]Toki, K., Shinohara, S., Tanikawa, T., Funaki, I., and Shamrai, K., “Preliminary Investigation of Helicon Plasma Source for Electric Propulsion Applications,” *28th. Int. Electric Propul. Conf.*, IEPC 03-0168, Toulouse, 17-21 Mar., 2003.

[12]Toki, K., Shinohara, S., Tanikawa, T., and Shamrai, K. P., “Feasible Study of Electrodeless Mangnetoplasmadynamic Acceleration,” *40th AIAA/ASME/SAE/ASEE Joint Propul. Conf. & Exhibit*, AIAA2004-3935, Lauderdale, 11-14 July, 2004.

[13]Ikeda, Y., Hada, T., Matsukiyo, S., Shinohara, S., and Toki, K., “Response of a Cylindrical Plasma to Time-Varying External Magnetic Field: Numerical Simulation Studies,” *29th Int. Electric Propul. Conf.*, IEPC-2005-177, Princeton, 31 Oct. 31-4 Nov., 2005.

[14]Toki, K., Shinohara, S., Tanikawa, T., and Shamrai, K., “Small Helicon Plasma Source for Electric Propulsion,” *Thin Solid Films*, Vol. 506-507, 26 May 2006, pp. 597-600.

[15]Shinohara, S., Hada, T., Motomura, T., Tanaka, K., Tanikawa, T., Toki, K., Tanaka, Y., and Shamrai, K., “Development of High-Density Helicon Plasma Sources and Their Applications,” *Phys. Plasmas*, Vol. 16, No. 5, May 2009, pp. 057104 1-10.

[16]Toki, K., Shinohara, S., Tanikawa, T., Hada, T., Funaki, I., Shamrai, K. P., Tanaka, Y., and Yamaguchi, A., “Plasma Acceleration of Compact Helicon Source Using RF Antennae,” J. *Plasma Fus. Res. SERIES*, Vol. 8, 2009, pp. 25-30.

[17]Nishida, H., Shinohara, S., Tanikawa, T., Hada, T., Funaki, I., Matsuoka, I, Shamrai, K. P., and Motomura, T., “Preliminary Study on Electrodeless Magneto-Plasma-Dynamic Thruster Using a Helicon Plasma Source,” *46th AIAA/ASME/SAE/ASEE Joint Propul. Conf. & Exhibit*, AIAA2010-7013, Nashville, 25-28 July, 2010.

[18]Matsuoka, T., Funaki, I., Nakamura, T., Yokoi, K., Nishida, H., Shamrai, K. P., Tanikawa, T., Hada, T., and Shinohara, S., “Scaling Laws of Lissajous Acceleration for Electrodeless Helicon Plasma Thruster,” *Plasma Fusion Res.*, Vol. 6, 2011, pp. 2406103 1-4.

[19]Jones, I. R., “A Review of Rotating Magnetic Field Current Drive and the Operation of the Rotamak as a Field-Reversed Configuration (ROTAMAK-FRC),” *Phys. Plasmas*, Vol. 6, No. 5, 1999, pp. 1950-1957.

[20]Matsuoka, T., Funaki, I., Rudenko, T. S., Shamrai, K. P., Satoh, S., Fujino, T., Nakamura, T., Yokoi, K., Nishida, H., Shinohara, S., Hada, T., and Tanikawa, T., “Progress in Development for Helicon Plasma Thrusters by Use of the Rotating Electric Field (Lissajous Acceleration),” 32nd *Int. Electric Propul. Conf.* (this conference), IEPC-2011-079, Wiesbaden, 11-15 Sept., 2011.

[21]Nakamura, T., Yokoi, K., Nishida, H., Shinohara, S., Funaki, I., Matsuoka, T., Tanikawa, T., Hada, T., Shamrai, K. P., and Rudenko, T. S., “Experimental Investigation of Plasma Acceleration by Rotating Electric Field for Electrodeless Plasma Thruster,“ 32nd *Int. Electric Propul. Conf.* (this conference), IEPC-2011-279, Wiesbaden, 11-15 Sept., 2011.

[22]Shinohara, S., and Tanikawa, “Development of Very Large Helicon Plasma Source,” *Rev. Sci. Instrum*., Vol. 75, No. 6, June 2004, pp. 1941-1946.

[23]Tanikawa, T., and Shinohara, S., "Large-Volume, Helicon-Plasma Source for Simulation Experiments of Space Plasmas," *Int. Cong. on Plasma Phys.*, Nice, 25-29 Oct., 2004, URL: http://hal.archives-ouvertes.fr/hal-00002013/en/.

[24]Shinohara, S., Takechi, S., and Kawai, Y., "Effects of Axial Magnetic Field and Faraday Shield on Characteristics of RF Produced Plasma Using Spiral Antenna," *Jpn. J. Appl. Phys.*, Vol. 35, Part I No. 8, Aug. 1996, pp. 4503-4508.

[25]Milroy, R. D., "A Numerical Study of Rotating Magnetic Fields as a Current Drive for Field Reversed Configurations," *Phys. Plasmas*, Vol. 6, No. 7, July 1999, pp. 2771-2779.

[26]Inomoto, M., "Plasma Acceleration by Using Rotating Magnetic Field," *IEEJ Trans. FM*, Vol. 128, No. 4, 2008, pp. 319-320 (in Japanese).

[27]Hudis, M., and Lidsky, L. M., "Directional Langmuir Probe," *J. Apply. Phys.*, Vol. 41, No. 12, Nov. 1970, pp. 5011-5017.

[28]Chung, K-S., Hutchinson, I. H., LaBombard, B., and Conn, R. W., "Plasma Flow Measurement along the Presheath of a Magnetized Plasma," *Phys. Fluids*, Vol. B 1, No. 11, Nov. 1989, pp. 2229-2238.

[29]Ando, A., Watanabe, T., Watanabe, T., Sato, R., Harata, K., Tobari, H., Hattori, K., And Inutake, "Evaluation of Mach Probe Characteristics and Measurement of High-Mach-Number Plasma Flow," *Thin Solid Films*, Vol. 506-507, May 2006, pp. 692-696.

[30]VORPAL, Ver. 4.2, Tech-X Corporation, Boulder, CO, 2010.

[31]Bering III, E. A., Chang Díaz, F. R., Squire, J. P., Glover, T. W., Carter, M. D., McCaskill, G. E., Longmier, B. W., Brukardt, M. S., Chancery, W. J., and Jacobson, V. T., "Observationof Single-Pass Ion Cyclotron Heating in a Trans-Sonic Flowing Plasma," *Phys. Plasmas*, Vol. 17, No. 4, April 2010, pp. 043509 1-19.

[32]Dodin, I. Y., Fisch, N. J., and Rax, J. M., "Ponderomotive Barrier as a Maxwell Demon," *Phys. Plasmas*, Vol. 11, Issue 11, Nov. 2004, pp. 5046-5064.

[33]Emsellem, G., "Development of a High Power Electrodeless Thruster," *29th Int. Electric Propul. Conf.*, IEPC-2005-156, Princeton, 31 Oct. 31-4 Nov., 2005.

[34]Tanikawa, T., and Shinohara, S., "Characteristics of Helicon-Plasma Produced Using a Segmented Multi-Loop Antenna II," *50th Annual Meeting of the Div. Plasma Phys., the American Phys. Soc.*, NP6.00018, Dallas, 17-21 Nov., 2008.